Unclassified

AD A102849

REPORT DOCUMENTATION PAGE		READ INSTRUCTIONS BEFORE COMPLETING FORM
1. Report Number AFOSR-81-0607	2. Govt Accession No. AD-A102849	3. Recipient's Catalog Number
4. Title (and Subtitle) NUMERICAL PREDICTION OF CONFINED TURBULENT VORTEX FLOWS.		5. Type of Report & Period Covered Progress Report 1980 - 1981.
		6. Performing Org. Report Number HIC 3601
7. Author(s) F. Boysan, J. Swithenbank		8. Contract or Grant Number AFOSR-79-0012
9. Performing Organization Name and Address University of Sheffield, Mappin Street, Sheffield S1 3JD, U.K.		10. Program Element, Project, Task Area & Work Unit Numbers 61102F 2308/A2
11. Controlling Office Name and Address Air Force Office of Scientific Research/NA, Building 410, Bolling Air Force Base, DC 20332		12. Report Date September 1980
		13. Number of Pages 18
14. Monitoring Agency Name and Address LEVEL II		15. Unclassified

16. & 17. Distribution Statement

Approved for public release; distribution unlimited.

18. Supplementary Notes

19. Key Words

Mathematical Modelling
Swirling Flow
Vortex Flow
Finite Difference
Swirl Burners

20. Abstract

Numerical predictions of turbulent vortex flow in cyclone chambers are made with the aid of a two-equation model of turbulence which entails the solution of elliptic differential equations of the transport of turbulence energy and its dissipation rate. The non-homogeneous and anisotropic nature of turbulence is accounted for by employing a two-viscosity concept. Reasonable agreement is obtained between the calculated axial and tangential velocity profiles and the experimental data available in the literature.

FORM 1473

Unclassified

department of chemical engineering and fuel technology

UNIVERSITY OF SHEFFIELD

Atch 4

NUMERICAL PREDICTION OF CONFINED TURBULENT VORTEX FLOWS

F. Boysan and J. Swithenbank

Department of Chemical Engineering and
Fuel Technology, University of Sheffield,
Sheffield, S1 3JD.

Sep[redacted]80

NUMERICAL PREDICTION OF CONFINED TURBULENT VORTEX FLOWS

F. Boysan and J. Swithenbank

Department of Chemical Engineering and Fuel Technology
University of Sheffield

Abstract

Numerical predictions of turbulent vortex flow in cyclone chambers are made with the aid of a two-equation model of turbulence which entails the solution of elliptic differential equations of the transport of turbulence energy and its dissipation rate. The non-homogeneous and anisotropic nature of turbulence is accounted for by employing a two-viscosity concept. Reasonable agreement is obtained between the calculated axial and tangential velocity profiles and the experimental data available in the literature.

Introduction

Cyclone dust separators, fluidic vortex amplifiers and swirl combustors are only a few of the many engineering applications of the cyclone chamber. The vortex motion in this device is created by the tangential introduction of the fluid into a cylindrical chamber with a single axial exit in one end plate. Numerous configurations are possible depending on the number and position of the tangential entry ports, the location of the axial exit and the length of diameter ratio of the cylindrical chamber. Despite its simple geometry, the aerodynamics of the cyclone chamber is extremely complicated. A typical flow pattern is depicted in Fig. 1 which is characterized by several annular zones of forward and reverse flow, entrainment of the fluid from the outside at the exit and the high degree of retention of swirl.

In the past there have been several experimental studies of the vortex structure in the cyclone chamber. Baluev and Troyankin [1] have reported measurements of the all three components of velocity in 23 designs with the aid of a calibrated five channel probe. Hot-wire anemometer measurements of not only the mean but also the fluctuating velocity components have been made

by Ustimenko and Bukhman [2]. Observations of the flow pattern in a cyclone chamber using smoke have been conducted by Smith [3], who also measured the axial and tangential time averaged velocity components using a cobra probe to determine direction and a special pilot-static to measure the magnitude. Unfortunately, vortex flows are extremely sensitive to disturbances created by probes [3,4,5] and hence these measurements are perhaps of questionable value. Non-intrusive optical diagnostic techniques have recently started to become available and at the time of writing of this paper LDA measurements in a vortex tube have been reported by Escudier et al [6].

The theoretical analysis of swirling flows on the other hand is extremely difficult and little progress in this area has so far been achieved. Apart from the fact that the governing equations are non-linear and strongly coupled, the structure of turbulence is non-homogeneous and anistropic, therefore, not suitable for analysis by closure hypotheses developed for quasilinear flows. Numerical solutions of laminar flow in a cyclone chamber have been obtained by Lilley and Vatistas [7]. However, the purpose of their efforts have been to demonstrate the capabilities of a certain numerical scheme rather than to arrive at quantitative conclusions about the structure of the flow.

The object of the present study is to provide numerical predictions of turbulent vortex flow in cyclone chambers and to investigate the applicability of the existing models of turbulence.

Mathematical Formulation

The equations required for the description of the aerodynamic pattern in cyclone chambers express the fluid flow balance of mass and momentum, and are given here in cylindrical co-ordinates (x, r, θ) best suited to the geometry of the problem. This approach is supported by experimental observations that the flow in cyclones with four or more tangential entries loses its three dimensional character at a short distance from the ports and becomes axially

symmetric. The derivatives with respect to the θ co-ordinate have been equated to zero.

Continuity

$$\frac{\partial}{\partial x}(ru) + \frac{\partial}{\partial r}(rv) = o \qquad (1)$$

x-momentum

$$\rho\left(v\frac{\partial u}{\partial r} + u\frac{\partial u}{\partial x}\right) = -\frac{\partial p}{\partial x} + \frac{1}{r}\frac{\partial}{\partial r}\left(r\mu\left[\frac{\partial u}{\partial r} + \frac{\partial v}{\partial x}\right]\right) + \frac{\partial}{\partial x}\left(2\mu\frac{\partial u}{\partial x}\right) \qquad (2)$$

r-momentum

$$\rho\left(v\frac{\partial v}{\partial r} + u\frac{\partial v}{\partial x} - \frac{w^2}{r}\right) = -\frac{\partial p}{\partial r} + \frac{1}{r}\frac{\partial}{\partial r}\left(2\mu r\frac{\partial v}{\partial r}\right) + \frac{\partial}{\partial x}\left(\mu\left[\frac{\partial u}{\partial r} + \frac{\partial v}{\partial x}\right]\right) - 2\mu\frac{v}{r^2} \qquad (3)$$

θ-momentum

$$\rho\left(v\frac{\partial w}{\partial r} + u\frac{\partial w}{\partial x} + \frac{vw}{r}\right) = \frac{1}{r}\frac{\partial}{\partial r}\left(\mu r^2\frac{\partial}{\partial r}\frac{w}{r}\right) + \mu\frac{\partial}{\partial r}\left(\frac{w}{r}\right) + \frac{\partial}{\partial x}\left(\mu\frac{\partial w}{\partial x}\right) \qquad (4)$$

In the above equations, u, v and w are the components of velocity in the x, r and θ directions respectively, p is the pressure, ρ is the density and μ is the viscosity.

It is assumed that these equations are valid for the present problem provided that all the flow variables and fluid properties are represented by the corresponding time-mean values. μ is now the effective viscosity which is the molecular viscosity augmented by the turbulent contribution. The distribution of the effective viscosity is determined by the 'turbulence model' employed.

Many models of turbulence exist, some involve the calculation of the effective viscosity from a prescribed length scale, the others require the solution of one or more partial differential equations. The two-equation k-ε model, which is of moderate complexity, has been extensively used by many

investigators and proven to be adequate over a wide range of flow situations. This model entails the solution of two transport equations of turbulence characteristics, namely the local energy of the fluctuating motion K and the energy dissipation rate ε. These equations can be written as:

$$\rho\left(v\frac{\partial K}{\partial r} + u\frac{\partial K}{\partial x}\right) = \frac{1}{r}\frac{\partial}{\partial r}\left(r\frac{\mu_t}{\sigma_K}\frac{\partial K}{\partial r}\right) + \frac{\partial}{\partial x}\left(\frac{\mu_t}{\sigma_K}\frac{\partial K}{\partial x}\right) + G_K - C_D\,\rho\,\varepsilon \qquad (5)$$

$$\rho\left(v\frac{\partial \varepsilon}{\partial r} + u\frac{\partial \varepsilon}{\partial x}\right) = \frac{1}{r}\frac{\partial}{\partial r}\left(r\frac{\mu_t}{\sigma_\varepsilon}\frac{\partial \varepsilon}{\partial r}\right) + \frac{\partial}{\partial x}\left(\frac{\mu_t}{\sigma_\varepsilon}\frac{\partial K}{\partial x}\right) + (C_1\,G - C_2\,\rho\,\varepsilon)\frac{\varepsilon}{K} \qquad (6)$$

Where σ_K and σ_ε are the turbulent Prandtl numbers for K and ε, and G is the rate of generation of K which is defined as:

$$G = \mu_t\left[2\left\{\left(\frac{\partial u}{\partial x}\right)^2 + \left(\frac{\partial v}{\partial r}\right)^2 + \left(\frac{v}{r}\right)^2\right\} + \left(\frac{\partial w}{\partial x}\right)^2 + \left(\frac{\partial u}{\partial r} + \frac{\partial v}{\partial x}\right)^2 + \left(\frac{\partial w}{\partial r} - \frac{w}{r}\right)^2\right] \qquad (7)$$

Solution of the above equations for K and ε allows the local turbulence and effective viscosities to be evaluated from:

$$\mu_t = C_\mu\,\rho\,K^2/\varepsilon \quad \text{and} \quad \mu_{eff} = \mu_t + \mu \qquad (8),\ (9)$$

respectively. The coefficients C_1, C_2, C_D, C_μ, σ_K and σ_ε are constants which are assigned the following values, $C_1 = 1.44$, $C_2 = 1.92$, $C_D = 1.0$, $C_\mu = 0.09$, $\sigma_K = 1.0$ and $\sigma_\varepsilon = 1.3$ as recommended by Launder, Priddin and Sharma [8].

Despite the success with which the K-ε model given by equations (5) and (6) has allowed prediction of numerous turbulent flows, its ability to reproduce the strong influence of swirl has not been sufficient. It has been suggested in the past that the effects of rotation can be accounted for by making the mixing length a function of a 'swirl' Richardson number [9,10]. This basic approach is not compatible with the K-ε model where the distribution of the length scale is obtained from the solution of differential transport equations rather than prescribed. A modification consistent with the two equation model has been proposed by Launder et al [8], which involves the

replacement of the constant C_2 in the transport equation of the energy dissipation rate by

$$C_2^* = C_2 \ (1 - C_3 \ Ri) \tag{10}$$

Where C_3 is an additional constant and Ri is the local Richardson number defined as follows

$$Ri = \frac{K^2}{\varepsilon^2} \ \frac{w}{r^2} \ \frac{\partial}{\partial r} (rw) \tag{11}$$

Furthermore, in view of the recent experimental results [11] which dispute the assumption of isotropy on which the K-ε model rests, a simple two-viscosity approach proposed by Lilley [12] is adopted in the present study. The effects of anisotropy are accomodated in the conservation of momentum equation in the θ-direction by employing an effective exchange coefficient related to the effective viscosity calculated from (9) by

$$\mu_{eff,w} = \mu_{eff}/\sigma_w$$

where, σ_w is a constant

Solution Procedure

The equations presented in the preceding section are elliptic in the x and r directions because they contain the second order derivatives with respect to both these directions. The solution procedure, therefore, needs two dimensional storage and requires iteration. Before an attempt is made to solve the equations however, they must be reduced into their finite difference analogues. This is achieved by integrating the equations over a computational cell. The resulting algebraic equations can be represented in the following common form:

$$\left(\sum_{i=N,S,E,W} A_i - S_p \right) \Phi_p = \sum_{i=N,S,E,W} A_i \Phi_i + S_u \tag{12}$$

Where the A's are the coefficients which contain the contributions from the convective and diffusive fluxes, S_u and S_p are the components of the linearized source term. The set of algebraic simultaneous equations (12) are solved by the SIMPLE algorithm of Patankar and Spalding [13]. This algorithm involves the solution of the momentum equations for a guessed pressure distribution to give a first estimate of the velocity fields. Corrections to the pressu.e and velocity fields are then obtained from the pressure equation of continuity. These corrections are such that the resulting velocities will satisfy continuity.

Boundary Conditions

Because of the elliptic nature of the equations, a complete description of the problem considered necessitates the specification of the boundary conditions at all the boundaries of the domain of integration.

In the near wall regions, the well known wall functions are matched with the algebraic equations (12) to preclude fine grid calculations in this region. The usual practice is to cut the link between the boundary and near-wall points by setting the appropriate coefficient to zero, and to insert the wall influence by way of the linearized source terms. The specific wall functions employed in the present study are

$$\tau_w = \frac{u_p}{y_p \chi^{-1}} \quad \frac{\mu y_p^+}{\ln (E Y_p^+)} \tag{13}$$

$$Y_p^+ = \rho (K_p C_\mu^{\frac{1}{2}})^{\frac{1}{2}} \frac{y_p}{\mu} \tag{14}$$

$$\varepsilon_p = (C_\mu^{\frac{1}{2}} K_p)^{3/2} / \chi y_p \tag{15}$$

Where, τ_w is the shear stress at the wall, u_p, K_p and ε_p are the velocity, turbulence energy and dissipation rate at the near wall node respectively, y_p is the distance from the wall, χ and E are constants.

The boundary conditions at the axis of symmetry are of the zero normal gradient type for all the variables except the radial and tangential components of velocity which are themselves zero there.

Although the conditions at the inlet are specified once and for all and do not need updating during the course of the solution procedure, those at the exit are not known beforehand. An analytical difficulty associated with confined vortex flows is their extreme sensitivity to downstream boundary conditions [14]. In order to mimimize the effects of the downstream conditions on the flow inside the cyclone chamber, the domain of integration is extended further downstream of the chamber exit. The boundary conditions imposed at this end are of the gradient type for all the dependent variables.

Results

The calculations were performed for a cyclone chamber of diameter $D = 0.25$ m, length $L = 0.386$ m and exit throat diameter $D_c = 0.1$ m. The fluid was assumed to be fed into the chamber through a circumferential slot, the width of which was adjusted so that the flow rate and the inlet velocities matched the experimental conditions reported by Ustimenko and Bukhman [2]. The ratio of tangential to radial velocity components at the inlet was of the order of 10. In order to preserve the stability of the numerical solution procedure and to obtain convergence for such high degrees of swirl, it was found necessary to reduce the under-relaxation parameters of all the three velocity components to 0.25. The number of iterations required was also in direct proportion with the degree of swirl. The calculations were performed on a 30 x 21 non-uniform grid in the x and r directions respectively.

Fig. 2 shows the vector plot of velocity distribution in the chamber predicted using the conventional K-ε model of turbulence. It can be seen that the incoming flow follows the chamber wall until the base plate is reached, where it changes direction and forms a reverse stream. The fluid leaves the chamber after a final change of direction without sucking any

fluid from the outside. A more realistic flow pattern is shown in Fig. 3 which is obtained by employing the two-viscosity approach including the Richardson number correction described in the foregoing sections. It is apparent from this vector plot and from the distribution of the streamlines given in Fig. 4 that the incoming stream does not change direction in the second half of the chamber, but the streamlines bend radially towards the axis of symmetry for a short distance before they become almost parallel to it and flow out of the chamber. This time, however, fluid is sucked into the cyclone chamber from the outside, which is in accord with the experimental observations [1,2].

The comparison between measured (2) and calculated axial velocity profiles are displayed in Fig. 5. It is interesting to note that all the calculated curves which correspond to the K-ε model, two-viscosity approach with and without Richardson number correction show fair agreement with the experimental data in the region $0.5\ R < r < R$, for all four axial locations. In the vicinity of the axis, however, the K-ε model fails to predict the reverse flow altogether. The two-viscosity model shows some reverse flow for $\sigma_w = 5$ and $C_3 = 0$, but the best agreement with the experimental data is obtained for $\sigma = 2.5$ and $C_3 = 10^{-3}$.

Fig. 6 shows the tangential velocity profiles both measured and calculated at the four axial locations. It is apparent that the K-ε model predictions do not reproduce even the qualitative features of the measured profiles except for the region in the extreme vicinity of the cylindrical wall and underestimate the degree of retention of the initial swirl. It is found that better qualitative agreement can be achieved when σ_w is increased. However, as seen from the figure, although for $\sigma_w = 5$ the predicted swirl velocities are well above the measured ones there is not enough reverse flow at the chamber exit. The best overall agreement is attained for $\sigma_w = 2.5$ and $C_3 = 10^{-3}$ as in the case of axial velocity profiles.

Finally, Fig. 7 displays the profiles of the kinetic energy of turbulence. The agreement between the data and the predicted curves is indeed poor. It is interesting to note that the K-ε model can reproduce the experimental profile for $r > 0.5\ R$, while the kinetic energy is grossly over-estimated both for $\sigma_w = 5.0$, $C_3 = 0$ and $\sigma_w = 2.5$, $C_3 = 10^{-3}$. This suggests that σ_w also may be a function of Richardson number and the K-ε model may apply after all in the region close to the wall of the chamber.

Concluding Remarks

Numerical predictions have been presented of turbulent vortex flow in cyclone chambers. The turbulence is modelled basically by the usual K-ε model. The transport equation for the dissipation rate of turbulence energy, however, was modified by making one of the constants a function of the local Richardson number. The anisotropic character of the turbulence was accounted for by employing a different effective viscosity for the θ-direction momentum equation. Although the constants σ_w and C_3 could be tuned so as to obtain reasonable agreement between the predicted and measured axial and tangential velocity profiles, the distribution of turbulence energy could not be reproduced.

On the other hand, since most of the measurements in cyclone chambers reported in the literature have been made by inseration of probes into the flow, it is difficult to judge whether the source of error is in the experiments or turbulence modelling. At this stage, therefore, one must conclude that detailed measurements of confined vortex flows by means of non-intrusive optical techniques are required urgently to validate an appropriate turbulence model.

Acknowledgements

This work was supported by the U.K. Science Research Council and USAF under contract AFOSR 80-0174.

References

1. Baluev, E.D. and Troyankin, V., 'Study of the Aerodynamic Structure of Gas Flow in a Cyclone Chember', Teploenergetika 14 (1), pp. 63-65, 1967.

2. Ustimenko, B.P. and Bukhman, M.A., 'Turbulent Flow Structure in a Cyclone Chamber', Teploenergetika 15 (2), pp. 64-67, 1968.

3. Smith, J.L., 'An Experimental Study of the Vortex in the Cyclone Separator', ASME J. Basic Eng., December 1962, pp. 602-608.

4. Holman, J.P. and Moore, G.D., 'An Experimental Study of Vortex Chamber Flow', ASME J. Basic Eng., 83, p. 632, 1961.

5. Swithenbank, J., Flow Visualization in Cyclone Chambers - Film. 1975.

6. Escudier, M.P., Bornstein, J. and Zehnder, N., 'Observations and LDA Measurements of Confined Turbulent Vortex Flow', J. Fluid Mech. 98, Part 1, pp. 49-63, 1980.

7. Lilley, D.G. and Vatistas, G., 'Flow Prediction in Cyclone Chambers', Paper presented at Combustion Institute/Canadian Section Meeting, Ottawa, 1978.

8. Launder, B.E., Priddin, C.H. and Sharma, B.I., 'The Calculation of Turbulent Boundary Layers on Spinning and Curved Surfaces', J. Fluids Eng., March 1977, p.231.

9. Bradshaw, P., "The Analogy Between Streamline Curvature and Bouyancy in Turbulent Shear Flow', J. Fluid. Mech., 36, p. 1007, 1971.

10. Prandtl, L., 'Collected Works', Springer-Verlag, Berlin. 1961.

11. Pratte, B.D. and Keffer, J.F., 'The Swirling Turbulent Jet', J. Basic Eng., 95, 1973.

12. Lilley, D.G., 'Prediction of Inert Turbulent Swirl Flows', AIAA Journal, 11, No. 7, p. 955, 1973.

13. Patankar, S.V. and Spalding D.B., 'A Calculation Procedure for Heat Mass and Momentum Transfer in Three Dimensional Parabolic Flows', Int. J. Heat Mass Transfer, 15, 1972.

14. Razgaitis, R. and Holmann J.P., 'A Survey of Heat Transfer in Confined Swirl Flows', presented at the Summer Seminar of the International Centre for Heat and Mass Transfer, Dubrovnik, Yugoslavia, August 1975.

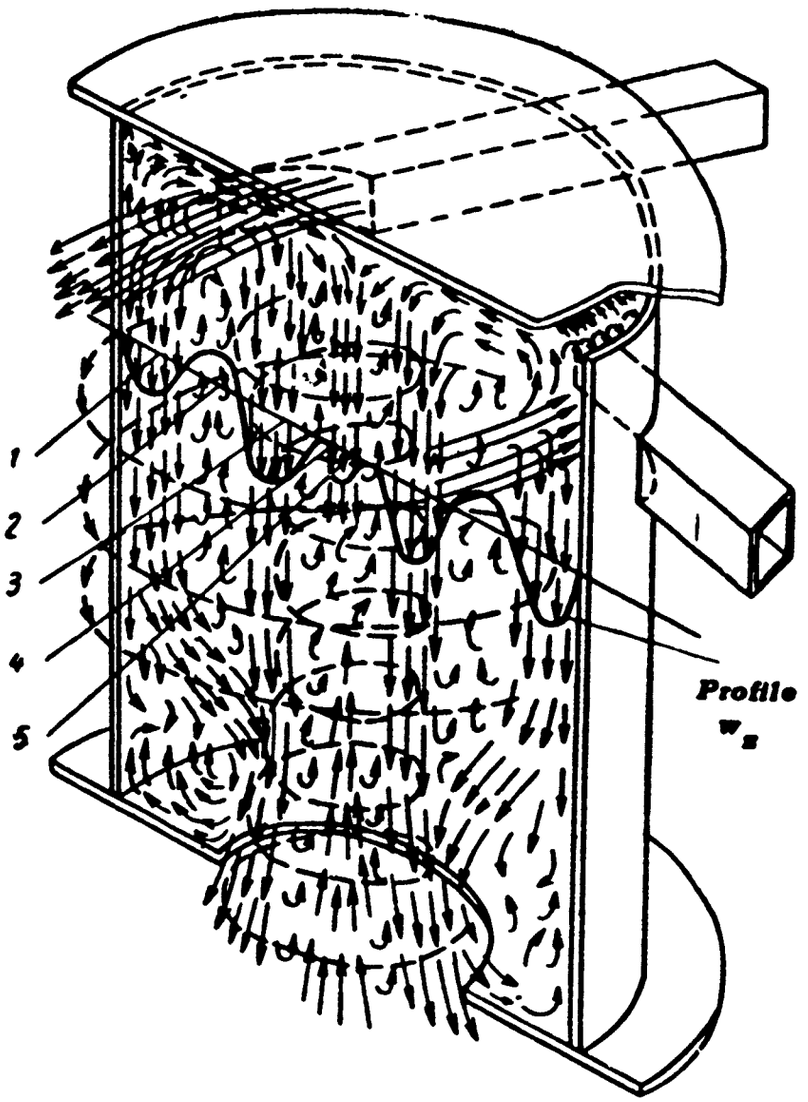

Pattern of gas flow in the cyclone chamber.
1-5-zones and flows.

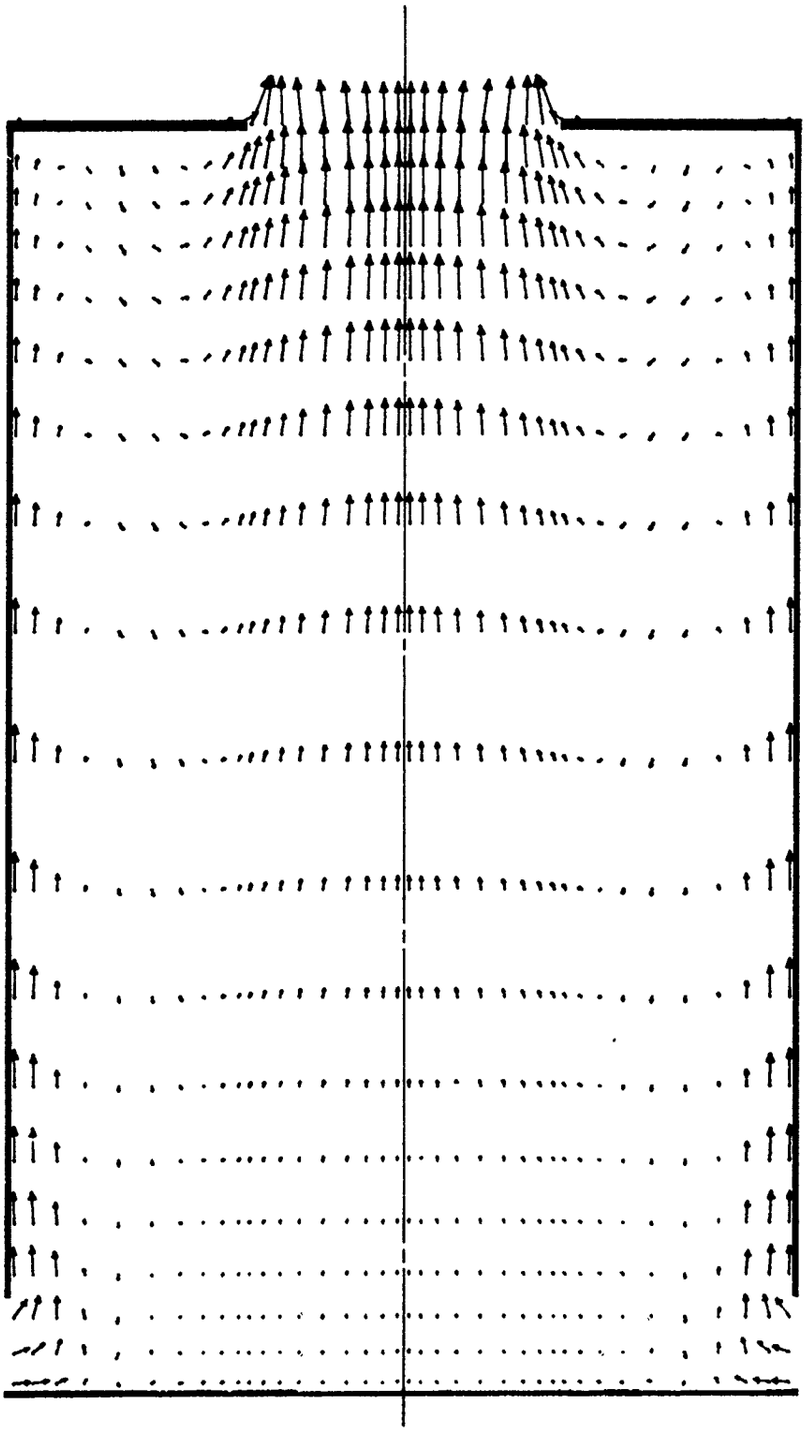

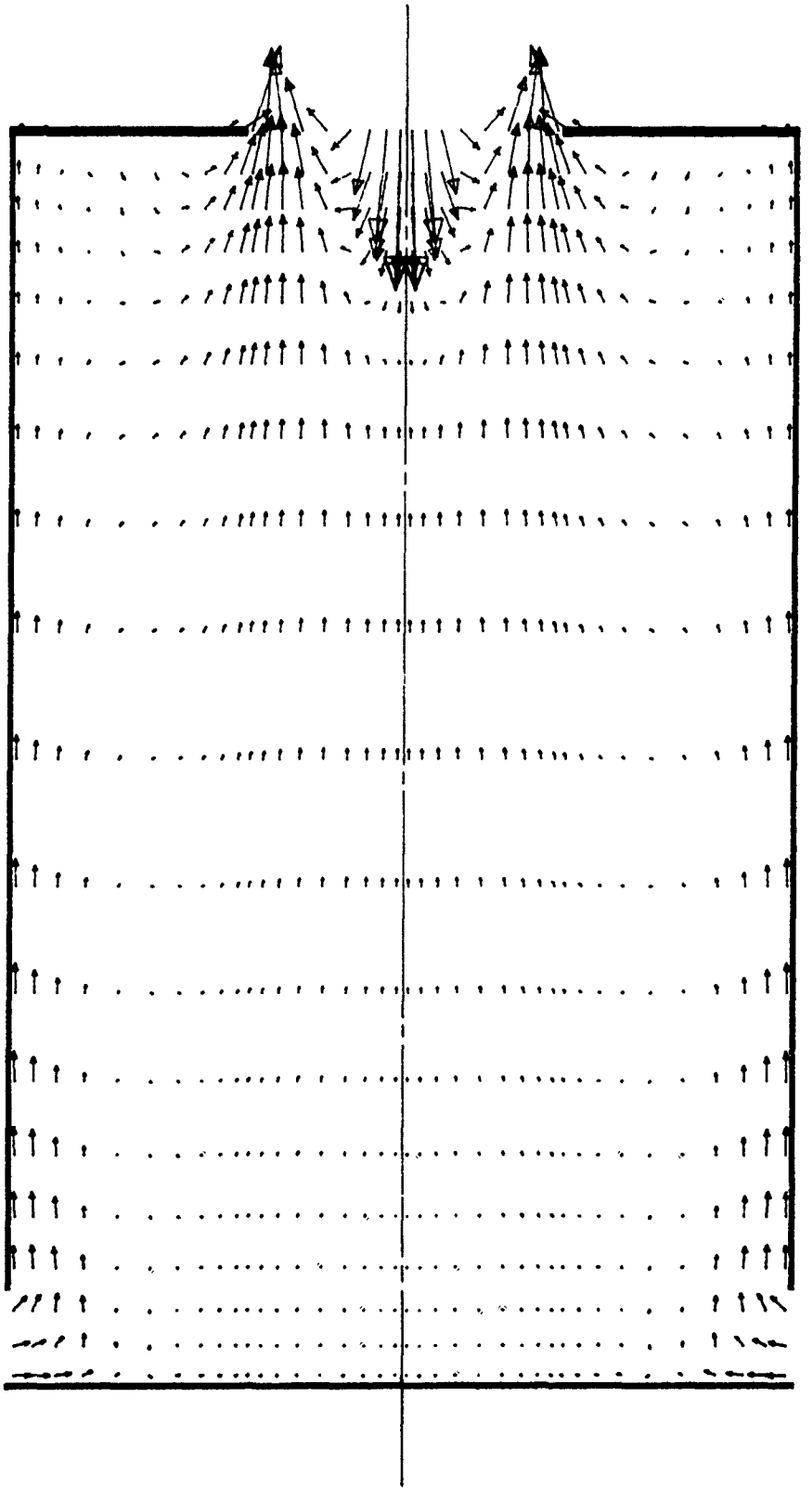

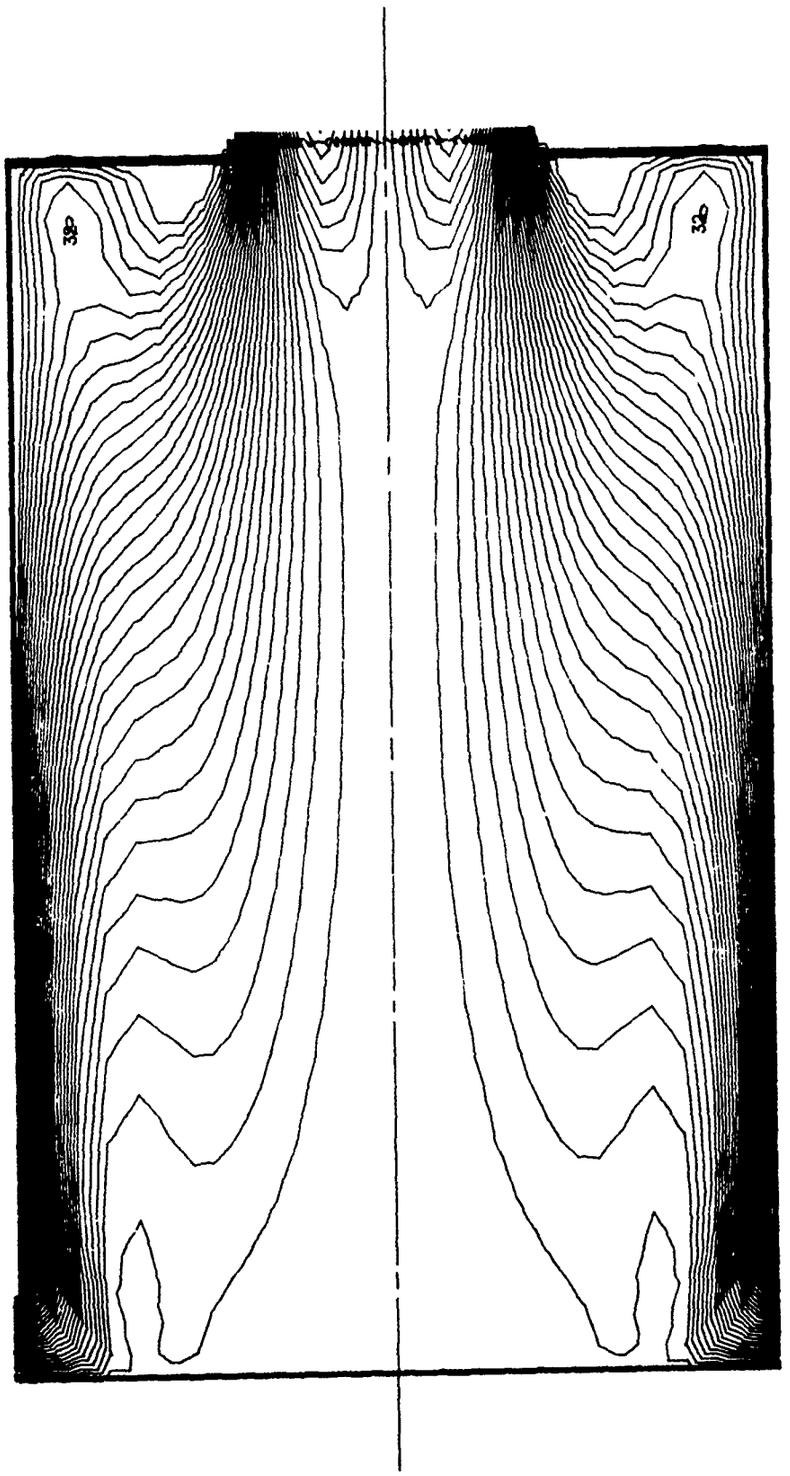
38
32

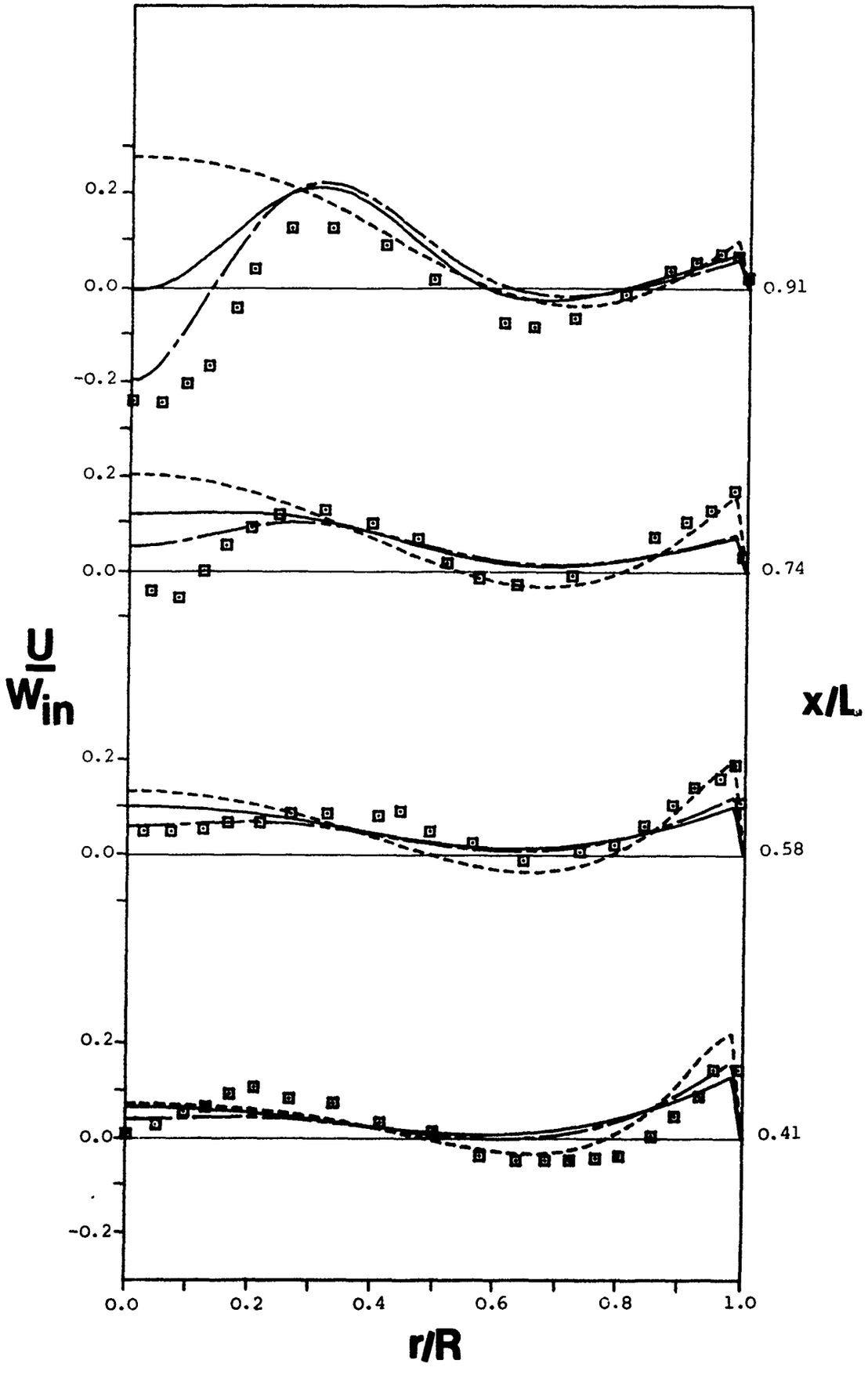
0.2
0.0
-0.2
0.91
0.74
0.58
0.41
U/W_in
x/L
0.0
0.2
0.4
0.6
0.8
1.0
r/R

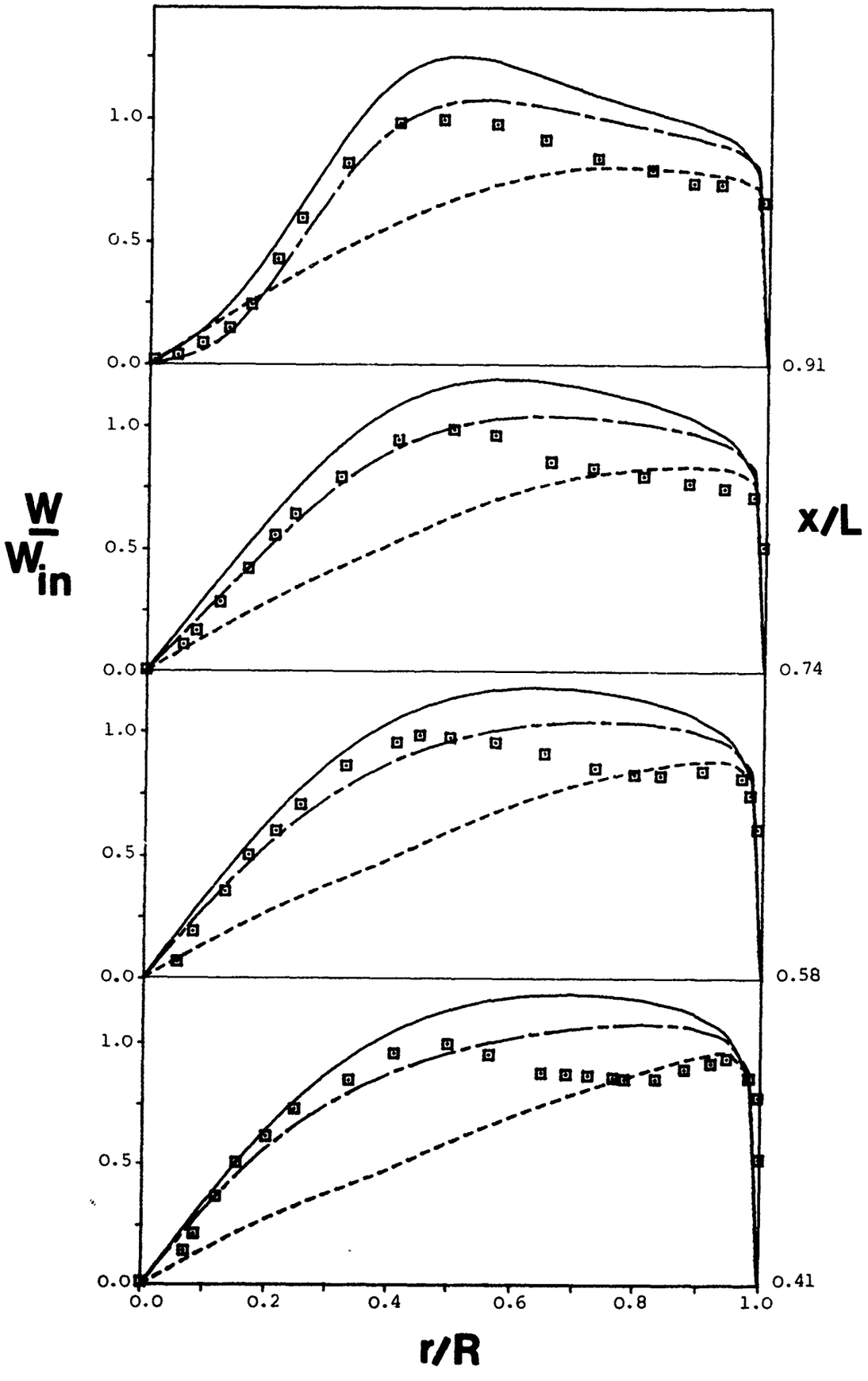
W/W_in
1.0
0.5
0.0
0.91
0.74
0.58
0.41
x/L
0.0
0.2
0.4
0.6
0.8
1.0
r/R

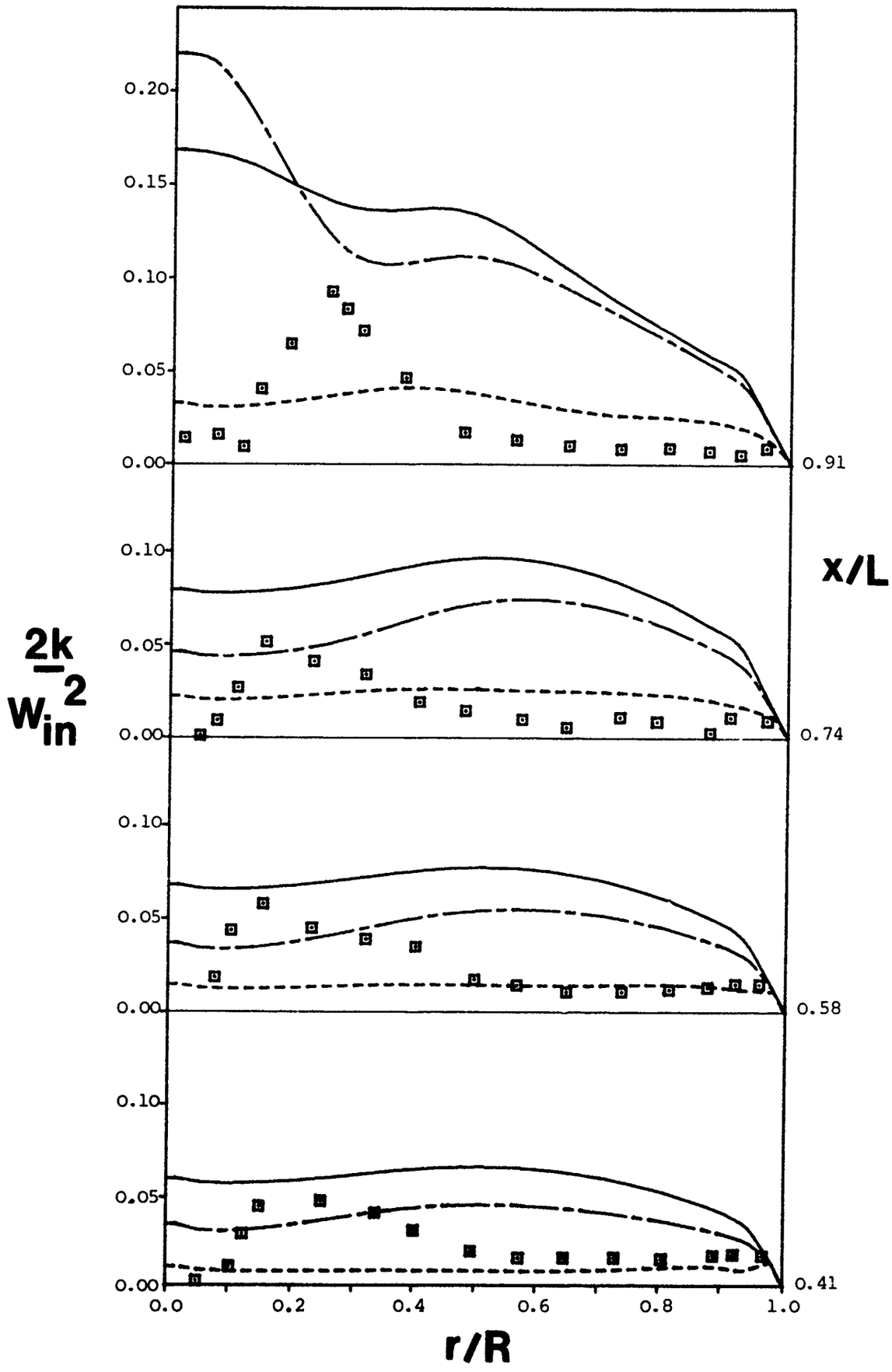
0.20
0.15
0.10
0.05
0.00
0.91
0.10
0.05
0.00
0.74
0.10
0.05
0.00
0.58
0.10
0.05
0.00
0.41
0.0
0.2
0.4
0.6
0.8
1.0
r/R
x/L
2k
W_in^2

Figure Captions

Fig. 1 Flow patterns observed in a cyclone chamber with four tangential entries and a single axial exit (from [2]).

Fig. 2 Velocity vectors in the cyclone chamber calculated using the k-ε model of turbulence.

Fig. 3 Calculated velocity vectors in the cyclone chamber for $\sigma_w = 2.5$, $c_3 = 10^{-3}$

Fig. 4 Calculated distribution of streamlines in the cyclone chamber for $\sigma_w = 2.5$, $c_3 = 10^{-3}$

Fig. 5 Comparison of measured and predicted axial velocity profiles at four downstream stations. ⊡ experiments, -----k-ε model, ——— k-ε model with σ_w=5 c_3=0.0, ——k-ε model with σ_w=2.5 c_3=10^{-3}

Fig. 6 Comparison of measured and predicted tangential velocity profiles in the cyclone (for legend see Fig. 5).

Fig. 7 Comparison of measured and predicted variation of kinetic energy of turbulence (for legend see Fig. 5).